The Journal of Experimental Biology 213, 2748-2754

doi:10.1242/jeb.042994

Review

‘It’s hollow’: the function of pores within myoglobin

Ayana Tomita[1,2,*,†], Ulrike Kreutzer[3], Shin-ichi Adachi[2,4], Shin-ya Koshihara[1,2] and Thomas Jue[3,†]

[1]Department of Chemistry and Materials Science, Tokyo Institute of Technology, 2-12-1 Oh-okayama, Meguro-ku, Tokyo, 152-8551, Japan, [2]Non-equilibrium Dynamics Project, ERATO/JST, 1-1 O-ho, Tsukuba, Ibaraki 305-0801, Japan, [3]Department of Biochemistry and Molecular Medicine, University of California Davis, CA 95616-8635, USA and [4]Photon Factory, Institute of Materials Structure Science, High Energy Accelerator Research Organization, 1-1 O-ho, Tsukuba, Ibaraki 305-0801, Japan

*Author for correspondence (atomita@chem.titech.ac.jp)
†These authors contributed equally to this work

Accepted 17 May 2010

Summary

Despite a century of research, the cellular function of myoglobin (Mb), the mechanism regulating oxygen (O_2) transport in the cell and the structure–function relationship of Mb remain incompletely understood. In particular, the presence and function of pores within Mb have attracted much recent attention. These pores can bind to Xe as well as to other ligands. Indeed, recent cryogenic X-ray crystallographic studies using novel techniques have captured snapshots of carbon monoxide (CO) migrating through these pores. The observed movement of the CO molecule from the heme iron site to the internal cavities and the associated structural changes of the amino acid residues around the cavities confirm the integral role of the pores in forming a ligand migration pathway from the protein surface to the heme. These observations resolve a long-standing controversy – but how these pores affect the physiological function of Mb poses a striking question at the frontier of biology.

Key words: oxygen, respiration, ligand migration, protein, laser, NMR, crystallography, seal.

Introduction

Over the years, comparative physiologists have investigated the biological adaptations that support life under a wide range of environmental conditions. In particular, the transport and utilization of oxygen have commanded special attention because aerobic metabolism plays such a central role in sustaining cellular bioenergetics and because many living organisms, such as marine mammals, endure long periods with low oxygen. Indeed, seals can plumb the ocean depth for up to 80 min without taking a breath and without exhibiting any sign of anaerobiosis (Butler and Jones, 1997). On land, elephant seals (*Mirounga angustirostris*) can spontaneously hold their breath (apnea) for about 10 min without relinquishing oxidative metabolism (Castellini et al., 1994; Le Boeuf et al., 2000).

The adaptations that can sustain physiological function under conditions of low oxygen cast insight into the mechanisms coordinating cardiac, vascular and metabolic regulation. For seals, apnea presents an opportune model for marine biologists to study these adaptations in response to the cessation of respiration: heart rate decreases to 40–50 beats min^{-1}, blood flow falls by 50% and both arterial and venous P_{O_2} values decline to 15–20 mmHg (Ponganis et al., 2006; Stockard et al., 2007). Yet, despite all these changes, blood lactate concentration, a hypoxemia marker, does not rise (Andrews et al., 1997; Castellini et al., 1986; Ponganis et al., 2006; Stockard et al., 2007). During a dive, marine mammals also rely on their O_2 store in Mb, which can reach almost 4 mmol l^{-1} (Butler and Jones, 1997; Ponganis et al., 2002; Scholander, 1940; Scholander et al., 1942). Through blood-flow reduction, downregulated metabolism, falling intracellular P_{O_2} that helps maintain a vascular-to-cellular O_2 gradient and the release of the Mb oxygen store, the seal has evolved a strategy to maintain aerobic metabolism during a breath hold. Experimental data show that Mb in the apneic juvenile elephant seal supports a large fraction of the total oxygen flux (Ponganis et al., 2008).

Aside from an O_2 storage function, Mb can also carry O_2 from the sarcolemma to the mitochondria in heart and skeletal muscle (Wittenberg and Wittenberg, 2003). In addition to the diffusive flux of free O_2, the translational diffusion of oxymyoglobin also provides an O_2 flux (Wyman, 1966). In the cell, the low solubility of O_2 and the low P_{O_2} imply that the Mb-bound O_2 concentration exceeds the free O_2 concentration. At the basal myocyte P_{O_2} of *ca*. 10 mmHg, the concentration of Mb-bound O_2 (260 µmol l^{-1}) in rat heart stands about 20 times higher than the level of free O_2 (13 µmol l^{-1}) (Masuda et al., 2008). Even though free O_2 diffuses more rapidly than Mb, the concentration difference between free O_2 and Mb-bound O_2 can still confer a significant role for Mb in contributing to the overall O_2 flux if Mb has sufficient diffusive mobility in the cell (Gros et al., 2010; Johnson et al., 1996). No theoretical or experimental evidence supports any direct transfer of O_2 from one myoglobin molecule to another in a ‘bucket brigade’ fashion (Gibson, 1959).

Plants also utilize proteins to facilitate intracellular O_2 transport. Leghemoglobin, a protein similar to myoglobin found in legume root nodules, has a tenfold greater oxygen affinity than that of Mb. It transports O_2 from the cell membrane of the central cells of the legume root nodule to the symbiosome, a membrane-bound organelle containing the bacterium *Rhizobium* and acting like the mitochondrion of muscle cells. The 10^5:1 ratio of leghemoglobin-bound O_2 to free O_2 implies that leghemoglobin has a predominant role in mediating the intracellular O_2 flux (Appleby, 1984).

Because of the substantial experimental evidence, scientists have justified closing the inquiry about Mb function. Thus, Mb is seen as simply providing a cellular O_2 store and facilitating O_2 diffusion

(Wittenberg, 1970). However, many creatures have an inadequate Mb O_2 reservoir to buffer against hypoxemia or ischemia (Chung and Jue, 1996). Even though *in vitro* evidence supports the theory of Mb-facilitated O_2 diffusion, recent translational diffusion measurements have not determined a Mb mobility sufficient to confer a significant contribution to the O_2 flux in rat myocardium or skeletal muscle (Lin et al., 2007b; Papadopoulos et al., 2001). However, because of its high concentration, Mb appears to have a predominant role in facilitating O_2 diffusion in seal myocytes (Lin et al., 2007a; Ponganis et al., 2008).

How intertidal animals utilize Mb to downregulate energy utilization and compensate for O_2 deficit during hypoxic stress in order to preserve functional integrity remains an open question (Hardewig et al., 1991; Hochachka and Guppy, 1987; Kleinschmidt and Weber, 1998; Weber and Pauptit, 1972). In particular, the lugworm *Arenicola marina* shows adaptations in the glycogenolysis and mitochondrial pathways leading to the formation of end-products such as opines, succinate and volatile fatty acids. It also exhibits a gradually decreasing rate of oxygen consumption as oxygen levels decline, well before the accumulation of anaerobic end-products (Grieshaber et al., 1994; Schöttler et al., 1983; Schöttler, 1987).

Despite the tomes of experimental data, the function of Mb still remains a mystery. In fact, O_2 does not bind exclusively to the heme, as often presumed, but can potentially bind to a number of other sites in Mb. These sites, as detected by x-ray crystallography and NMR studies, bind to Xe as well as other ligands and, by implication, can form a pathway for O_2 to reach the heme from the protein surface (Schoenborn et al., 1965; Tilton et al., 1984; Tilton and Kuntz, 1982). Indeed, a recent x-ray crystallographic study has followed the CO migration into Xe-binding cavities of sperm whale Mb. CO induces a structural expansion as it interacts with the pores to mimic the action of a 'protein lung' during CO passage (Tomita et al., 2009). The observed CO migration helps trace the route that O_2 can take from the surface through a maze of seemingly impenetrable amino acids to the heme (Case and Karplus, 1979; Perutz and Mathews, 1965). But, at the same time, the function of these pores remains a puzzle.

Comparative physiologists should consider taking a lead to open again the inquiry into Mb function. Without a well-defined cellular function under specific physiological conditions, the elegance of the biophysical structural analysis can never achieve a level of biological significance. However, for physiologists to take an effective lead, they must gather informed perspectives and look through the lens of structural biology to gain novel insights.

Protein structure and function

In 1959, just 50 years ago, John Kendrew and Max Perutz succeeded finally in capturing the three-dimensional X-ray crystallographic structure of Mb at 2 Å resolution and of hemoglobin (Hb) at 5.5 Å resolution (Kendrew et al., 1960; Perutz et al., 1960). Their accomplishment records in the annals of science an indelible human journey that history will recount again and again (Dickerson, 2009; Rossman, 2009; Strandberg, 2009). After years of dogged determination, Kendrew and Perutz ushered in a new era in exploring protein structure and gave scientists an indispensable X-ray crystallographic tool to understand some fundamental principles in molecular biology regarding how the sequence of amino acids encodes for protein function and how the protein structure modulates function to meet the complex physiological demands of the cell.

In choosing sperm whale Mb as his model, Kendrew selected an abundant muscle protein with well-defined O_2 binding characteristics and with a propensity to crystallize. Once Perutz had overcome the formidable phase problem in X-ray crystallographic analysis with heavy atom derivatives, Kendrew used the approach to solve the Mb structure at 6 Å resolution (Kendrew et al., 1958). At 6 Å resolution, however, the analysis could not confirm Linus Pauling's prediction of α-helical structure in the polypeptide segments (Pauling et al., 1951). So, in August 1959, Kendrew's team spent all night collecting an electron-density map to calculate the structure at 2 Å resolution. As the data started to roll-in, the team saw the 6 Å sausage-like features revealing α-helical structure. Next day, at the celebration party, Sir Lawrence Bragg, the founder of the X-ray crystallographic principles for structural determination, dragged one party attendee after another to look at the contoured Plexiglas sheets of the 2 Å resolution Mb map. He pointed exultantly down the E helix and exclaimed: "Look! It's hollow! It's hollow!" (Dickerson, 2009).

Half a century has since passed, and many consider the Mb tale a closed chapter in science. Yet, to the contrary, new experimental observations have now begun to rattle our complacency about the accepted Mb model. A mouse without any Mb survives and functions with no apparent physiological deficits (Flogel et al., 2005; Garry et al., 1998). Mb does not appear to have any significant role in regulating steady-state myocardial respiration (Chung et al., 2006; Kreutzer et al., 1998). Its translational diffusion appears too slow to compete effectively with free O_2 (Lin et al., 2007a; Lin et al., 2007b; Papadopoulos et al., 1995; Papadopoulos et al., 2001). Instead of one hollow pocket to accommodate the heme, which binds covalently to O_2 and other ligands, many hydrophobic pockets dot the folded Mb landscape. These pockets can also bind to ligands.

Even though Perutz and Kendrew ushered in the era of crystallographic protein structure determination, structure derives meaning only in relationship to function. Yet, the function of the Mb, especially with respect to the hollow pockets, remains a mystery.

Ligand pathway to the heme

Conventionally, biochemistry envisions the 16 kDa monomeric Mb binding O_2 at the Fe (II) heme with a dissociation constant (K_D) of *ca.* 1 μmol l^{-1}. CO binds to Mb with a K_D of *ca.* 0.1 μmol l^{-1}, whereas NO binds with an even higher affinity. By contrast, cytochrome oxidase has an estimated K_m of <0.1 μmol l^{-1} for O_2, whereas Hb has a corresponding K_D of 25 μmol l^{-1} (Antonini and Brunori, 1971; Carver et al., 1992). Even though spectrophotometric assays can easily measure O_2 binding, the space-filling model of Mb based on the X-ray crystal structure shows no clear path for the diatomic molecules to diffuse from the protein surface to the heme (Perutz and Mathews, 1965). Only through side-chain fluctuations can a passage begin to open for ligands to diffuse to and from the active heme site.

The creation of random passages for O_2 diffusion into the heme pocket seems inconsistent with the defined spatial arrangement in Mb. The heme intercalates into a specific region of apomyoglobin to form the holoenzyme. On the proximal side, the His93 (F8: the eighth amino acid residue on the F helix) binds covalently to the heme iron. From the distal pocket (DP), ligands can bind to the heme (Fig. 1). Highly conserved amino acid residues, including the His64 (E7), form the distal pocket. Nevertheless, the crystal structure of Mb does not show any direct pathway of oxygen migration connecting between the binding site and the protein

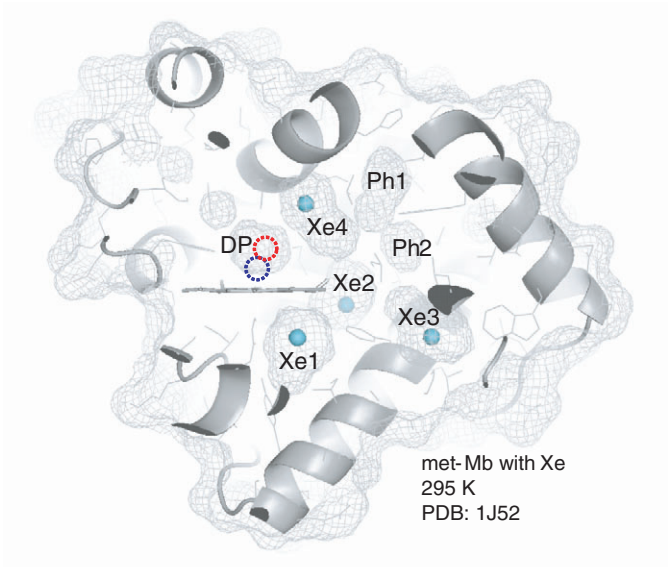

Fig. 1. The structure of Mb showing the different internal cavities: four xenon-binding sites (Xe1–Xe4), two Phantom sites (Ph1 and Ph2) and the distal pocket (DP) above the heme plane and near the distal histidine (E64). A mesh outlines the molecular surface, which encloses the internal cavities. The blue dotted circle denotes the ligand binding position, and the red dotted circle traces the primary docking site.

surface. The absence of a discernible pathway for O_2 entry has posed a long-standing mystery (Perutz and Mathews, 1965).

Fig. 1 also localizes other pockets in Mb, Xe1–Xe4. The surfaces of the internal cavities are marked by a mesh. In addition to the Xe pockets, other cavities, Phantom1 (Ph1) and Phantom2 (Ph2), also exist. These cavities appear highly conserved and are found in sperm whale Mb and horse heart Mb. Yellow fin tuna and sea hare Mb have additional cavities. Molecular-dynamic simulations have proposed that transient protein fluctuations can open pathways for ligands to diffuse to the heme. A prominent pathway allows ligands to move into the DP, and the rotation of the distal His64 (E7) creates the final channel for ligand binding to the heme (Bolognesi et al., 1982; Perutz, 1989). Other researchers have suggested alternative pathways involving the B, G and H helices (Elber and Karplus, 1987; Huang and Boxer, 1994).

Indeed, photo-dissociation experiments have provided data to map the migration pathway (Olson and Phillips, 1996). Upon photo-irradiation, CO dissociates from MbCO with a high quantum efficiency of ~1 (Gibson, 1956). After CO dissociates from the heme, it either rebinds to the heme iron or escapes into the solvent. The movement of the photolysed CO can then trace the ligand migration pathway. Using optical absorption at 436 nm, studies have followed the rebinding rate of the CO molecule to Mb 10^{-6} s and 10^{3} s after photo-dissociation in solution at 40 and 350 K and have identified four different rebinding processes below 215 K (Austin et al., 1973; Austin et al., 1975). Indeed, multi-intermediate states exist along with three CO binding sites in the distal pocket (Austin et al., 1973; Austin et al., 1975). Some of the photolysed carbon monoxide (CO*) binding sites also bind to Xe (Brunori et al., 2000; Tilton et al., 1984). In fact, Kendrew's lab first noted that Mb can actually bind to Xe (Schoenborn et al., 1965).

Xe pockets

Researchers have posited that these Xe cavities might link with the transient fluctuations to form the ligand migration pathway (Tilton et al., 1984). Indeed, X-ray crystallography at cryogenic temperatures has detected photolysed CO trapped at the primary docking site below the glass transition temperature (<160 K) (Hartmann et al., 1996; Schlichting et al., 1994; Teng et al., 1994; Teng et al., 1997). At cryogenic temperatures, ligand becomes trapped at an intermediate state. Using a rapid cooling method, in which the crystal is rapidly cooled down to 90 K from 160 K under photo-irradiation, X-ray crystallography detects photolysed CO trapping to the Xe1 and Xe4 sites in wild-type and mutant Mb (Chu et al., 2000; Ostermann et al., 2000).

The CO molecule can localize at several xenon-binding cavities between 10^{-9}–10^{-3} s at *ca.* 300 K, as observed in time-resolved Laue crystallography of wild-type and mutant MbCO (Schmidt et al., 2005; Schotte et al., 2003; Schotte et al., 2004; Srajer et al., 1996; Srajer and Champion, 1991). Given the electron density, the analysis infers that CO moves from the primary docking site in the distal heme pocket (DP) to Xe1 and Xe4. Picosecond time-resolved crystallography of mutant L29F MbCO (where Leu29 is replaced by Phe29) reveals a highly strained intermediate structure at 100 ps and successfully visualizes how the correlated side-chain motion of His64 and Phe29 sweeps the photolysed CO molecule out of the distal pocket to Xe4 (Schotte et al., 2003).

Ligand migration and the Xe pockets

In order to map experimentally the ligand migration pathways in Mb, cryogenic X-ray crystallographic investigations using a novel photo-irradiation scheme with a high-repetition pulsed laser has followed the CO movement in sperm whale Mb (Tomita et al., 2009). More than 25 datasets collected at 100 K, 120 K and 140 K form the basis of the crystallographic analysis. These high-resolution, 1.2 Å, measurements at cryogenic temperatures enable the visualization of the CO migration from the heme iron site to the different internal cavities of Mb. As the electron densities of the CO molecule in four xenon-binding sites increase slowly with time, the other internal cavities (Ph1 and Ph2) close to the Xe2 and Xe4 sites show no corresponding change in electron density. Because the crystal structures observed by X-ray crystallography are the average structures of a large number of Mb molecules in the crystal, the occupancy of the CO molecule in each cavity corresponds to the population of Mb molecules in a particular intermediate structure.

In addition, microspectroscopic measurement of the MbCO crystal under the pulsed-laser illumination conditions at 120 K confirms the photo-dissociation of the CO molecule from the heme iron (Tomita et al., 2009). The optical absorption spectral change around the visible region (500–700 nm) indicates that the photo-dissociated CO converts Mb to its deoxy form.

CO migrates into a cavity in the lower part of the heme plane (Xe1) and in the back of the distal pocket (Xe4) after 300 min of laser irradiation at 120 K (Tomita et al., 2009). Accumulation of CO molecules in the Xe1 cavity has been reported previously by time-resolved and cryogenic crystallographic studies (Chu et al., 2000; Ostermann et al., 2000; Schmidt et al., 2005; Schotte et al., 2003; Srajer et al., 1996). It is noteworthy that time-resolved and cryogenic crystallography of wild-type MbCO did not capture the electron density of the CO molecule in the Xe4 cavity, probably owing to the low occupancy and/or high mobility of the CO molecule in the Xe4 cavity above 120 K (Chu et al., 2000; Schotte et al., 2004). Instead, by using Mb mutants in which the Leu29 position is replaced by Phe, Trp or Tyr, a CO molecule was trapped in the Xe4 cavity by stabilizing the free-energy level of the Xe4

cavity (Bourgeois et al., 2003; Bourgeois et al., 2006; Ostermann et al., 2000; Schotte et al., 2003).

Other features emerge at the Xe2 cavity at 450 min after pulsed-laser pumping. Regarding the Xe2 cavity, the pulsed-laser experiments have provided the first direct evidence of time-dependent evolution of electron densities of the CO molecule in the Xe2 cavity, which implicates its involvement in the CO migration channel (Tomita et al., 2009). The Xe3 cavity is partially occupied by a water molecule before the start of the pulsed-laser illumination. The increased electron density in the Xe3 cavity can arise from a combination of a photo-dissociated CO molecule from the DP and water molecule from the external solvent. However, the experiments have detected amino acid movements around the Xe3 cavity (Trp7, Leu137 and His82) observed. Consequently, it remains possible that the route from the distal pocket to the Xe3 cavity involving the Xe1, Xe2 and Xe4 cavities is the major ligand migration pathway in Mb under cryogenic conditions.

Breathing motion

The coordinated change of the amino acid residues in photolysed Mb becomes more prominent at 140 K. Fig. 2 shows the conformational change in the Mb molecule before and after photo-irradiation at 140 K. The residues involved in the gating motions are as follows: Leu29, His64 and Val68 (between the distal pocket and the Xe4 cavity), Leu69, Leu72 and Ile111 (between the Xe4 and Xe2 cavities), Leu76 and Phe138 (between the Xe2 and Xe3 cavities), Leu89 and Phe138 (between the Xe2 and Xe1 cavities) and Trp7, His82 and Leu137 (between the Xe3 cavity and the solvent). Fig. 3 shows a key map of the ligand migration in Mb. The superposed Mb structures before laser illumination (orange) and after 750 min laser illumination (yellow) at 140 K are shown with emphatic coordinates of the gating motion of amino acid residues. Emphatic coordinates are calculated from the coordinates of Mb before and after laser irradiation at 140 K. $X_{\text{emphatic1}}=X_{750\text{min}}+\Delta X$, $X_{\text{emphatic2}}=X_{750\text{min}}+2\Delta X$, $\Delta X=X_{750\text{min}}-X_{\text{Laseroff}}$. Here, X_{Laseroff} and $X_{750\text{min}}$ are atom coordinates of before-laser illumination and after 750 min of laser illumination at 140 K. This unveils the details of structural deformation of cavities and the gating motions of the surrounding amino acid residues.

The kinetic model indicates that the migration of the CO molecule into a cavity induces a structural deformation, which promotes the opening of the gates in the CO migration channel. When the CO leaves the cavity, it expands back to its original volume.

Comparison with molecular-dynamic simulations

The route from the distal pocket to the Xe3 cavity *via* Xe1, Xe2 and Xe4 agrees with the ligand migration pathway derived from the molecular-dynamics simulation (Bossa et al., 2004; Cohen et al., 2006; Elber and Karplus, 1987). Based on the simulation, Elber and Karplus suggest several pathways that involve internal cavities similar to Xe cavities. Their simulation proposes five ligand exits as follows: EF helix and N terminal, A/E helix, AB/G helix, proximal histidine and CD helix. In the major trajectory, CO must pass the major barrier residues of Leu72, Trp14, Leu76, Leu135, Met131, Val10 and Trp7. The exit is located in the neighborhood of Trp7. Four additional exits are located as follows: between Val17 and Thr70, near His24, between His93 and Ser92, and around Leu49. However, not all trajectories follow the same diffusive path to reach the exit.

The Elber and Karplus simulation assumes that a ligand hops randomly to a few sites in Mb. At each site, the ligand remains trapped for a significant time, before it hops to another cavity. Through these hopping motions, the ligand binds to the heme or leaves the protein. The simulation employs an enhanced sampling method: Mb starts out with 60 CO molecules with initial positions in the heme pocket. The simulation then counts CO collisions with the protein residues. These residues match the gate residues identified in the pulsed-laser experiments (Tomita et al., 2009).

Cohen and colleagues have also reported several pathways using the implicit ligand sampling method (Cohen et al., 2006). These pathways consist of DP, Xe1, Xe2, Xe3, Xe4 and other cavities. The pathway from the distal pocket to the Xe3 cavity involving the Xe2 and Xe4 cavities also agrees with the pulsed-laser results (Tomita et al., 2009). Bossa et al. have shown in their molecular dynamics calculation that the CO molecule remains in Ph cavities for a very short time compared with CO in the Xe cavities (Bossa

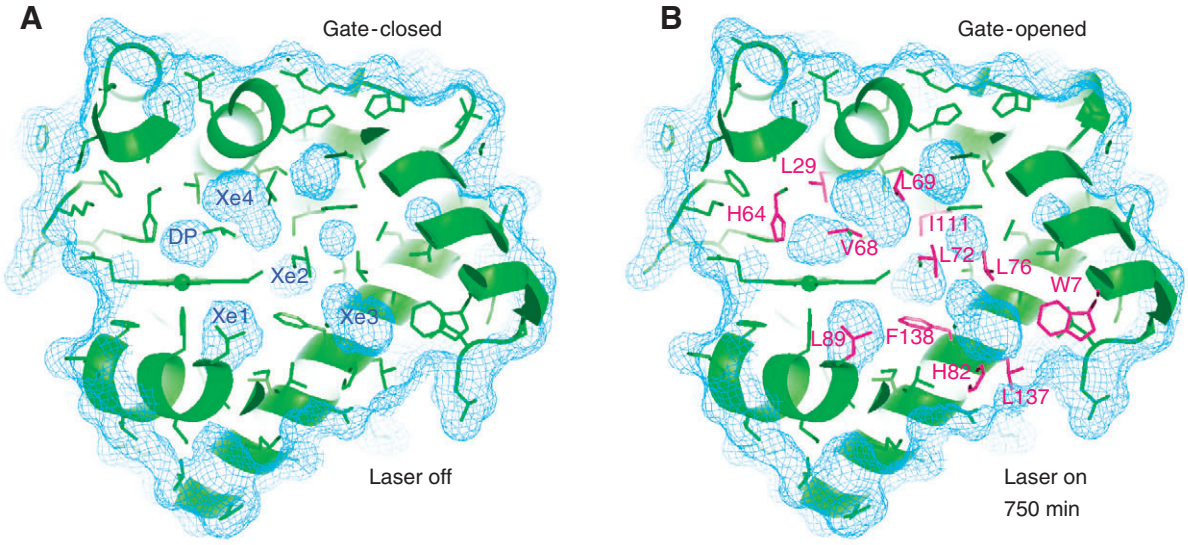

Fig. 2. Structure of MbCO at 140 K (A) before laser illumination and (B) after 750 min of laser illumination. The surfaces of the internal cavities are shown by the mesh. The residues involved in the gating motions are highlighted.

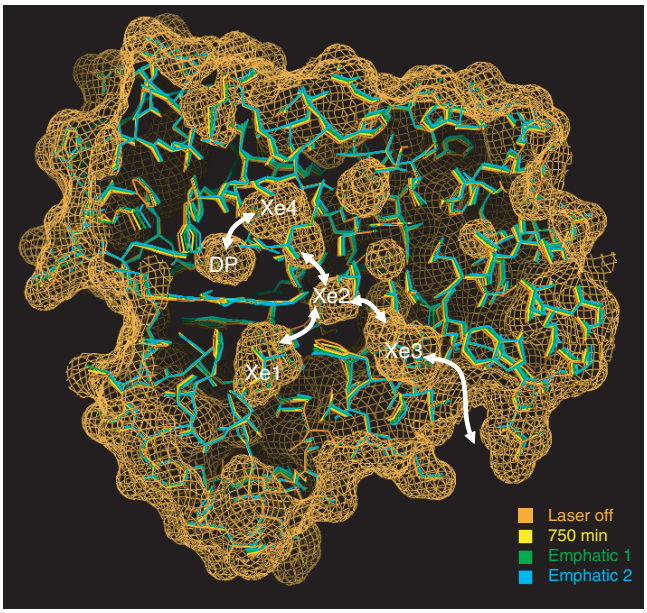

Fig. 3. Breathing motion of myoglobin: the superposed Mb structures before laser illumination (orange) and after 750 min of laser illumination (yellow) at 140 K are shown, with emphatic coordinates (green and cyan) of gating motion of amino acid residues. Emphatic coordinates are calculated from the coordinates of Mb before and after laser irradiation at 140 K. $X_{emphatic1}=X_{750min}+\Delta X$, $X_{emphatic2}=X_{750min}+2\Delta X$, $\Delta X=X_{750min}-X_{Laseroff}$. Here, $X_{Laseroff}$ and X_{750min} are atom coordinates of before-laser illumination and after 750 min of laser illumination at 140 K. The surfaces of the internal cavities are shown by the mesh. The movements of amino acid residues between the cavities are shown by white arrows.

et al., 2004). If the migration process into the Ph cavity is quick, and the ligand encounters shallow energy potentials, then the pulsed-laser experiments cannot easily detect these trapped intermediate states. The results agree with previous studies, which do find CO migrating to the Ph1 and Ph2 cavities but cannot exclude a direct pathway via the His64 gate (Bossa et al., 2004; Cohen et al., 2006).

The structural analysis clearly shows that the time-dependence of the electron density of the CO molecule in the Xe1, Xe2 and Xe4 cavities correlates with the change in the estimated volume of each cavity (Tomita et al., 2009). As the CO molecule migrates into a cavity, it induces a structural expansion due to steric interaction, which then promotes the self-opening of the CO migration channel by an induced fit. The kinetic potential barriers between the cavities are no longer defined statically but instead tuned dynamically by the ligand migration itself (Austin et al., 1975; Fenimore et al., 2002). This picture should be further examined by mapping the potential of the mean force (Cohen et al., 1972).

Thermal fluctuation

X-ray crystallographic analysis can establish both a spatial arrangement of atomic positions and fluctuations, as reflected in the mean-square displacement of the atom, $\langle x^2\rangle$. If the X-ray scattering intensity from each atom is multiplied by a Gaussian function, $\exp(-B\sin^2\theta/\lambda^2)$, where θ is the Bragg angle and λ is the wavelength of the X-ray; and B is defined as the atomic temperature factor, B-factor, or Debye–Waller factor, $B=8\pi^2\langle x^2\rangle$. Then, individual atomic $\langle x^2\rangle$ values will show variation depending on their fluctuation and their position in the protein tertiary structure. The relative magnitudes of the different atomic $\langle x^2\rangle$ values will correlate with structural features. Smaller B-factors correspond to rigidly bound atoms, either by covalent or non-covalent interaction. Average B-factors of main-chain atoms without laser and with 750 min of pulsed-laser irradiation at 140 K are coincident with the result of the atomic mean-square displacement analysis, which reflects exactly the tertiary structural features of the Mb molecule (Frauenfelder et al., 1979; Petsko and Ringe, 1984).

No major difference in B-factors of amino acid residues was observed around cavities between the laser-off state and the laser-on state after 750 min of laser irradiation. However, B-factor or amino acid motion increases at residues with large displacements. Focusing on the individual B-factor of each atom, an increased B-factor is observed at the edge of the residues. According to the movement of the His64 residue, the atomic B-factor rises notably in the imidazole ring of histidine. This feature is also found in the Phe138 that resides between the Xe2 and Xe3 cavities. Because the crystal structures are the average structure of a large number of Mb molecules in the crystal, the residue could be distributed around opened and closed conformations, and the B-factor could increase by superposing the particular intermediate structures.

Other functions of Mb pores

It appears that Mb pores linked to transient fluctuations create pathways for ligands to migrate from the protein surface to the heme. These pathways do not appear in the three-dimensional static structure but reveal themselves in modeling simulations and movement of photoactivated CO in laser experiments. At any given moment, the heme binds to one molecule of O_2, but, depending upon the O_2 affinity and occupancy at the other sites, Mb might carry additional O_2, resulting in a stoichiometry greater than 1:1.

This might have particular significance for diving mammals or animals enduring prolonged periods of hypoxic stress because the solubility of O_2 is quite low (Johnson et al., 1996). In the myocardium, the basal P_{O_2} of 10 mmHg in myocytes represents only about 13 μmol l^{-1} O_2. In mammals, Mb concentration usually ranges from 200–400 μmol l^{-1} (Masuda et al., 2008). Seal muscle has up to 3.8 mmol l^{-1} Mb (Butler and Jones, 1997; Ponganis et al., 2008). Relative to basal-state free O_2, Mb has a 25–500 times higher O_2 carrying capacity. If the pores can also carry O_2, Mb has an even higher O_2 carrying capacity. Given the predominant role of Mb-facilitated O_2 diffusion in seal muscle, the additional O_2 carrying capacity would enhance the capacity of marine mammals to maintain aerobic metabolism during a dive and of intertidal-zone animals to tolerate hypoxic stress (Grieshaber et al., 1994; Lin et al., 2007a; Lin et al., 2007b; Ponganis et al., 2008).

The provocative supposition that Mb has a higher O_2 carrying capacity than the 1:1 ratio specified by the heme:O_2 ratio requires experimental verification with modern instrumentation. In early measurements of Hb or blood oxygen content, the oxygen released from the heme by $Fe(CN)_6$ (ferricyanide) oxidation showed a stoichiometric ratio of heme:O_2 (Peters, 1912; Scholander, 1960). The literature does not report comparable Mb experiments. However, these Hb experiments might not have detected any contribution from protein pores because, even though Fe oxidation will release the O_2 from the heme, it will not necessarily affect the bound O_2 in the pores. Oxidized Hb (metHb) shares structural features similar to those of HbO_2 and can still have pockets with similar O_2 affinity (Perutz and Mathews, 1965). Moreover, because early investigators focused on developing field instrumentation to measure oxygen content in blood, they had already assumed a heme:O_2 stoichiometry and could have easily overlooked the telltale signs of another source of bound O_2 (Roughton et al., 1943).

The existence of Mb pores suggests that the Mb could potentially carry other molecules. In invertebrates, the oxygen transport protein hemocyanin can carry non-allosterically lipids and hormones in addition to O_2 (Cunningham et al., 1999; Jaenicke et al., 2010). Indeed, early experiments have hinted at a fatty acid transport role for Mb. These experiments detected ^{14}C oleic acid binding to a rat heart cytosolic fraction of 16 kDa, ascribed to Mb (Gloster and Harris, 1977). The binding to fatty acid exhibits on a per-mole basis a modest dissociation constant (K_D) of 12.2 to 48 μmol l^{-1} (Gloster, 1977; Gloster and Harris, 1977; Gotz et al., 1994). Unfortunately, other studies refuted the findings (Glatz and Veerkamp, 1983; Said and Schulz, 1984).

Recently, ^1H NMR experiments have detected the interaction of palmitate (PA) with metmyoglobin cyanide (MbCN), a surrogate model of MbO_2. These experiments have detected a selective change in the 8-heme methyl signal intensity, consistent with an apparent K_D of 43 μmol l^{-1}. In the presence of Mb, palmitate exhibits a higher solubility than in buffer alone (Sriram et al., 2008). Oleic acid elicits a similar change. Moreover, MbO_2 has a higher fatty acid affinity than deoxy Mb (T. Jue, unpublished observations).

A significant fatty acid interaction with Mb would raise questions about the monolithic viewpoint that only fatty acid binding protein (FABP) traffics fatty acid in the cell (Glatz and van der Vusse, 1989). Even though FABP has a higher affinity for fatty acid than Mb, Mb exists in a significantly higher concentration than FABP in the cell. Moreover, the differential K_D of MbO_2 and deoxyMb provides a convenient mechanism for dissociating fatty acid for mitochondrial metabolism in contrast to the complex release mechanism for FABP (Corsico et al., 2004). Nevertheless, the attractive hypothesis that Mb might serve to transport fatty acid must also await additional experiments that will measure the relative contribution of fatty acid transport by myoglobin and by FABP (Moore et al., 1993).

Perspective

Despite many decades of research and the era of protein structural determination opened by Kendrew and Perutz, many questions still surround the function of Mb. The fundamental relationship between Mb structure and function still stands as an unresolved issue in biology. In Mb and most likely in other proteins, pores exist. For Mb, these pores can accommodate Xe and other ligands and form part of the integrative pathway that leads O_2 from the protein to the heme. For other proteins, the functional relevance of pores remains uncertain. How these pores facilitate cellular function, bind to other molecules and regulate respiration as well as other physiological functions poses a set of challenging questions to biologists.

Acknowledgements

We acknowledge gratefully the editorial guidance and collegiality of Michael Berenbrink and thank Tokushi Sato, Shunsuke Nozawa, Kouhei Ichiyanagi, Hirohiko Ichikawa, Matthieu Chollet, Fumihiro Kawai, Sam-Yong Park, Takahisa Yamato and Takayuki Tsuduki for invaluable scientific discussions. The experimental work described in the article was performed under the approval of the Photon Factory Program Advisory Committee (PF-PAC 2004S1-001).

References

Andrews, R. D., Jones, D. R., Williams, J. D., Thorson, P. H., Oliver, G. W., Crocker, D. E., Costa, D. P. and Le Boeuf, D. J. (1997). Heart rates of Northern elephant seals while diving at sea and resting on the beach. *J. Exp. Biol.* **200**, 2083-2095.

Antonini, E. and Brunori, M. (1971). *Hemoglobin and Myoglobin in Their Reactions with Ligands*. Amsterdam: Elsevier/North Holland.

Appleby, C. A. (1984). Leghemoglobin and rhizobium respiration. *Annu. Rev. Plant Physiol.* **35**, 443-478.

Austin, R. H., Beeson, K., Eisenstein, L., Frauenfelder, H., Gunsalus, I. C. and Marshall, V. P. (1973). Dynamics of carbon monoxide binding by heme proteins. *Science* **181**, 541-543.

Austin, R. H., Beeson, K. W., Eisenstein, L., Frauenfelder, H. and Gunsalus, I. C. (1975). Dynamics of ligand binding to myoglobin. *Biochemistry* **14**, 5355-5373.

Bolognesi, M., Cannillo, E., Ascenzi, P., Giacometti, G. M., Merli, A. and Brunori, M. (1982). Reactivity of ferric Aplysia and sperm whale myoglobins towards imidazole. X-ray and binding study. *J. Mol. Biol.* **158**, 305-315.

Bossa, C., Anselmi, M., Roccatano, D., Amadei, A., Vallone, B., Brunori, M. and Di Nola, A. (2004). Extended molecular dynamics simulation of the carbon monoxide migration in sperm whale myoglobin. *Biophys. J.* **86**, 3855-3862.

Bourgeois, D., Vallone, B., Schotte, F., Arcovito, A., Miele, A. E., Sciara, G., Wulff, M., Anfinrud, P. and Brunori, M. (2003). Complex landscape of protein structural dynamics unveiled by nanosecond Laue crystallography. *Proc. Natl. Acad. Sci. USA* **100**, 8704-8709.

Bourgeois, D., Vallone, B., Arcovito, A., Sciara, G., Schotte, F., Anfinrud, P. A. and Brunori, M. (2006). Extended subnanosecond structural dynamics of myoglobin revealed by Laue crystallography. *Proc. Natl. Acad. Sci. USA* **103**, 4924-4929.

Brunori, M., Vallone, B., Cutruzzola, F., Travaglini-Allocatelli, C., Berendzen, J., Chu, K., Sweet, R. M. and Schlichting, I. (2000). The role of cavities in protein dynamics: crystal structure of a photolytic intermediate of a mutant myoglobin. *Proc. Natl. Acad. Sci. USA* **97**, 2058-2063.

Butler, P. J. and Jones, D. R. (1997). Physiology of diving of birds and mammals. *Physiol. Rev.* **77**, 837-899.

Carver, T. E., Brantley, R. E., Jr, Singleton, E. W., Arduini, R. M., Quillin, M. L., Phillips, G. N., Jr and Olson, J. S. (1992). A novel site-directed mutant of myoglobin with an unusually high O_2 affinity and low autooxidation rate. *J. Biol. Chem.* **267**, 14443-14450.

Case, D. A. and Karplus, M. (1979). Dynamics of ligand binding to heme proteins. *J. Mol. Biol.* **132**, 343-368.

Castellini, M. A., Costa, D. P. and Huntley, A. (1986). Hematocrit variation during sleep apnea in elephant seal pups. *Am. J. Physiol.* **251**, R429-R431.

Castellini, M. A., Milsom, W. K., Berger, R. J., Costa, D. P., Jones, D. R., Castellini, J. M., Rea, L. D., Bharma, S. and Harris, M. (1994). Patterns of respiration and heart rate during wakefulness and sleep in elephant seal pups. *Am. J. Physiol.* **266**, R863-R869.

Chu, K., Vojtchovsky, J., McMahon, B. H., Sweet, R. M., Berendzen, J. and Schlichting, I. (2000). Structure of a ligand-binding intermediate in wild-type carbonmonoxy myoglobin. *Nature* **403**, 921-923.

Chung, Y. and Jue, T. (1996). Cellular response to reperfused oxygen in the postischemic myocardium. *Am. J. Physiol.* **271**, H687-H695.

Chung, Y., Huang, S. J., Glabe, A. and Jue, T. (2006). Implication of CO inactivation on myoglobin function. *Am. J. Physiol. Cell Physiol.* **290**, C1616-C1624.

Cohen, J., Arkhipov, A., Braun, R. and Schulten, K. (2006). Imaging the migration pathways for O2, CO, NO, and Xe inside myoglobin. *Biophys. J.* **91**, 1844-1857.

Cohen, J. S., Hagenmaier, H., Pollard, H. and Schechter, A. N. (1972). Proton magnetic resonance study of the histidine residues of sperm whale and horse myoglobins. *J. Mol. Biol.* **71**, 513-519.

Corsico, B., Liou, H. L. and Storch, J. (2004). The alpha-helical domain of liver fatty acid binding protein is responsible for the diffusion-mediated transfer of fatty acids to phospholipid membranes. *Biochemistry* **43**, 3600-3607.

Cunningham, M., Gomez, C. and Pollero, E. (1999). Lipid binding capacity of spider hemocyanin. *Exp. Zool.* **284**, 368-373.

Dickerson, R. E. (2009). Chapter 2, Myoglobin: a whale of a structure. *J. Mol. Biol.* **392**, 10-23.

Elber, R. and Karplus, M. (1987). Multiple conformational states of proteins: a molecular dynamics analysis of myoglobin. *Science* **235**, 318-321.

Fenimore, P. W., Frauenfelder, H., McMahon, B. H. and Parak, F. G. (2002). Slaving: solvent fluctuations dominate protein dynamics and functions. *Proc. Natl. Acad. Sci. USA* **99**, 16047-16051.

Flogel, U., Laussmann, T., Godecke, A., Abanador, N., Schafers, M., Fingas, C. D., Metzger, S., Levkau, B., Jacoby, C. and Schrader, J. (2005). Lack of myoglobin causes a switch in cardiac substrate selection. *Circ. Res.* **96**, e68-e75.

Frauenfelder, H., Petsko, G. A. and Tsernoglou, D. (1979). Temperature-dependent X-ray diffraction as a probe of protein structural dynamics. *Nature* **280**, 558-563.

Garry, D. J., Ordway, G. A., Lorenz, J. N., Radford, N. B., Chin, E. R., Grange, R. W., Bassel-Duby, R. and Williams, R. S. (1998). Mice without myoglobin. *Nature* **395**, 905-908.

Gibson, Q. H. (1956). An apparatus for flash photolysis and its application to the reactions of myoglobin with gases. *J. Physiol.* **134**, 112-122.

Gibson, Q. H. (1959). The kinetics of reactions between haemoglobins and gases. *Progr. Biophys. Biophys. Chem.* **9**, 2-53.

Glatz, J. F. and van der Vusse, G. J. (1989). Intracellular transport of lipids. *Mol. Cell Biochem.* **88**, 37-44.

Glatz, J. F. C. and Veerkamp, J. H. (1983). A radiochemical procedure for the assay of fatty-acid binding by proteins. *Anal. Biochem.* **132**, 89-95.

Gloster, J. (1977). Studies on fatty-acid binding characteristics of myoglobin and Z-protein. *J. Mol. Cell. Cardiol.* **9**, 15.

Gloster, J. and Harris, P. (1977). Fatty-acid binding to cytoplasmic proteins of myocardium and red and white skeletal-muscle in rat-possible new role for myoglobin. *Biochem. Biophys. Res. Comm.* **74**, 506-513.

Gotz, F. M., Hertel, M. and Groschelstewart, U. (1994). Fatty-acid-binding of myoglobin depends on its oxygenation. *Biol. Chem. Hoppe Seyler* **375**, 387-392.

Grieshaber, M. K., Hardewig, I., Kreutzer, U. and Pörtner, H. O. (1994). Physiological and metabolic responses to hypoxia in invertebrates. *Rev. Physiol. Biochem. Pharmacol.* **125**, 43-147.

Gros, G., Wittenberg, B. and Jue, T. (2010). Myoglobin's old and new clothes: from molecular structure to function in living cells. *J. Exp. Biol.* **213**, 2713-2725.

Hardewig, I., Addink, A. D. F., Grieshaber, M. K., Pörtner, H. O. and Van den Thillart, G. (1991). Metabolic rates at different oxygen levels determined by direct

and indirect calorimetry in the oxyconformer *Sipunculus nudus*. *J. Exp. Biol.* **157**, 143-160.
Hartmann, H., Zinser, S., Komninos, P., Schneider, R. T., Nienhaus, G. U. and Parak, F. (1996). X-ray structure determination of a metastable state of carbonmonoxy myoglobin after photodissociation. *Proc. Natl. Acad. Sci. USA* **93**, 7013-7016.
Hochachka, P. W. and Guppy, M. (1987). *Metabolic Arrest and the Control of Biological Time*. Cambridge, MA: Harvard University Press.
Huang, X. and Boxer, S. G. (1994). Discovery of new ligand binding pathways in myoglobin by random mutagenesis. *Nat. Struct. Biol.* **1**, 226-229.
Jaenicke, E., Foell, R. and Decker, H. (2010). Spider hemocyanin binds ecdysone and 10-OH-ecdysone. *J. Biol. Chem.* **274**, 34267-34271.
Johnson, R. L., Jr, Heigenhauser, G. J. F., Hsia, C. C. W., Jones, N. L. and Wagner, P. D. (1996). Determinants of gas exchange and acid-base balance during exercise. In *Exercise: Regulation and Integration of Multiple Systems*, vol. 12 (ed. L. B. Rowell and J. Shepherd), pp. 515-584. New York: Oxford University Press.
Kendrew, J. C., Bodo, G., Dintzis, H., Parrish, R. G., Wyckoff, H. and Phillips, D. C. (1958). A threedimensional model of the myoglobin molecule obtained by X-ray analysis. *Nature* **181**, 662-666.
Kendrew, J. C., Dickerson, R. E., Strandberg, B. E., Hart, R. G., Davies, D. R., Phillips, D. C. and Shore, V. C. (1960). Structure of myoglobin: a three-dimensional Fourier synthesis at 2 Å resolution. *Nature* **185**, 422-427.
Kleinschmidt, T. and Weber, R. E. (1998). Primary structures of Arenicola marina isomyoglobins: molecular basis for functional heterogeneity. *Biochim. Biophys. Acta* **1383**, 55-62.
Kreutzer, U., Mekhamer, Y., Tran, T. K. and Jue, T. (1998). Role of oxygen in limiting respiration in the in situ myocardium. *J. Mol. Cell. Cardiol.* **30**, 2651-2655.
Le Boeuf, B. J., Crocker, D. E., Grayson, J., Gedamke, J., Webb, P. M., Blackwell, S. B. and Costa, D. P. (2000). Respiration and heart rate at the surface between dives in northern elephant seals. *J. Exp. Biol.* **203**, 3265-3274.
Lin, P. C., Kreutzer, U. and Jue, T. (2007a). Anisotropy and temperature dependence of myoglobin translational diffusion in myocardium: implication on oxygen transport and cellular architecture. *Biophys. J.* **92**, 2608-2620.
Lin, P. C., Kreutzer, U. and Jue, T. (2007b). Myoglobin translational diffusion in myocardium and its implication on intracellular oxygen transport. *J. Physiol.* **578**, 595-603.
Masuda, K., Truscott, K., Lin, P. C., Kreutzer, U., Chung, Y., Sriram, R. and Jue, T. (2008). Determination of myoglobin concentration in blood-perfused tissue. *Eur. J. Appl. Physiol.* **104**, 41-48.
Moore, K. K., Cameron, P. J., Ekeren, P. A. and Smith, S. B. (1993). Fatty acid-binding protein in bovine longissimus-dorsi muscle. *Comp. Biochem. Physiol. B Biochem. Mol. Biol.* **104**, 259-266.
Olson, J. S. and Phillips, G. N., Jr (1996). Kinetic pathways and barriers for ligand binding to myoglobin. *J. Biol. Chem.* **271**, 17593-17596.
Ostermann, A., Waschipky, R., Parak, F. G. and Nienhaus, G. U. (2000). Ligand binding and conformational motions in myoglobin. *Nature* **404**, 205-208.
Papadopoulos, S., Jurgens, K. D. and Gros, G. (1995). Diffusion of myoglobin in skeletal muscle cells – dependence on fibre type, contraction and temperature. *Pflügers Arch. Eur. J. Physiol.* **430**, 519-525.
Papadopoulos, S., Endeward, V., Revesz-Walker, B., Jurgens, K. D. and Gros, G. (2001). Radial and longitudinal diffusion of myoglobin in single living heart and skeletal muscle cells. *Proc. Natl. Acad. Sci. USA* **98**, 5904-5909.
Pauling, L., Corey, R. B. and Branson, H. R. (1951). The structure of proteins: two hydrogen-bonded helical configurations of the polypeptide chain. *Proc. Natl. Acad. Sci. USA* **37**, 205-211.
Perutz, M. F. (1989). Myoglobin and haemoglobin: role of distal residues in reactions with haem ligands. *Trends Biochem. Sci.* **14**, 42-44.
Perutz, M. F. and Mathews, F. S. (1965). An X-ray study of azide methaemoglobin. *J. Mol. Biol.* **21**, 199-202.
Perutz, M. F., Rossman, M. G., Cullis, A. F., Muirhead, H., Will, G. and North, A. C. T. (1960). Structure of haemoglobin. A three-dimensional Fourier synthesis at 5.5-Å resolution, obtained by X-ray analysis. *Nature* **185**, 416-422.
Peters, R. A. (1912). Chemical nature of specific oxygen capacity in haemoglobin. *J. Physiol.* **44**, 131-149.
Petsko, G. A. and Ringe, D. (1984). Fluctuations in protein structure from X-ray diffraction. *Annu. Rev. Biophys. Bioeng.* **13**, 331-371.
Ponganis, P. J., Kreutzer, U., Sailasuta, N., Knower, T., Hurd, R. and Jue, T. (2002). Detection of myoglobin desaturation in Mirounga angustirostris during apnea. *Am. J. Physiol. Regul. Integr. Comp. Physiol.* **282**, R267-R272.
Ponganis, P. J., Knower-Stockard, T., Levenson, D. H., Berg, I. and Baranov, E. A. (2006). Cardiac output and muscle blood flow during rest-associated apneas of elephant seals. *Comp. Biochem. Physiol. A Physiol.* **144**, 105-111.
Ponganis, P. J., Kreutzer, U., Stockard, T. K., Lin, P. C., Sailasuta, N., Tran, T. K., Hurd, R. and Jue, T. (2008). Blood flow and metabolic regulation in seal muscle during apnea. *J. Exp. Biol.* **211**, 3323-3332.
Rossman, M. G. (2009). Chapter **3**, Recollection of the events leading to the discovery of the structure of hemoglobin. *J. Mol. Biol.* **392**, 23-32.
Roughton, F. J. W. and Scholander, P. F. (1943). Micro gasometric estimation of the blood gases. I. Oxygen. *J. Biol. Chem.* **148**, 541-550.
Said, B. and Schulz, H. (1984). Fatty-acid binding-protein from rat-heart-the fatty-acid binding-proteins from rat-heart and liver are different proteins. *J. Biol. Chem.* **259**, 1155-1159.
Schlichting, I., Berendzen, J., Phillips, G. N., Jr and Sweet, R. M. (1994). Crystal structure of photolysed carbonmonoxy-myoglobin. *Nature* **371**, 808-812.
Schmidt, M., Nienhaus, K., Pahl, R., Krasselt, A., Anderson, S., Parak, F., Nienhaus, G. U. and Srajer, V. (2005). Ligand migration pathway and protein dynamics in myoglobin: a time-resolved crystallographic study on L29W MbCO. *Proc. Natl. Acad. Sci. USA* **102**, 11704-11709.
Schoenborn, B. P., Watson, H. C. and Kendrew, J. C. (1965). Binding of xenon to sperm whale myoglobin. *Nature* **207**, 28-30.
Scholander, P. F. (1940). Experimental investigations on the respiratory function in diving mammals and birds. *Hvalradets Skr.* **22**, 1-131.
Scholander, P. F. (1960). Oxygen transport through hemoglobin solutions. *Science* **131**, 585-590.
Scholander, P. F., Irving, L. and Grinnell, S. W. (1942). Aerobic and anaerobic changes in seal muscles during diving. *J. Biol. Chem.* **142**, 431-440.
Schotte, F., Lim, M., Jackson, T. A., Smirnov, A. V., Soman, J., Olson, J. S., Phillips, G. N., Jr, Wulff, M. and Anfinrud, P. A. (2003). Watching a protein as it functions with 150-ps time-resolved x-ray crystallography. *Science* **300**, 1944-1947.
Schotte, F., Soman, J., Olson, J. S., Wulff, M. and Anfinrud, P. A. (2004). Picosecond time-resolved X-ray crystallography: probing protein function in real time. *J. Struct. Biol.* **147**, 235-246.
Schöttler, U. (1987). Weitere Untersuchungen zum anaeroben Energiestoffwechsel des Polychaeten. *Arenicola marina L. Zool. Beitr.* **30**, 141-152.
Schöttler, U., Wienhausen, G. and Zebe, E. (1983). The mode of energy production in the lugworm *Arenicola marina* at different oxygen concentrations. *J. Comp. Physiol. B Biochem. Syst. Environ. Physiol.* **149**, 547-555.
Srajer, V. and Champion, P. M. (1991). Investigations of optical line shapes and kinetic hole burning in myoglobin. *Biochemistry* **30**, 7390-7402.
Srajer, V., Teng, T., Ursby, T., Pradervand, C., Ren, Z., Adachi, S., Schildkamp, W., Bourgeois, D., Wulff, M. and Moffat, K. (1996). Photolysis of the carbon monoxide complex of myoglobin: nanosecond time-resolved crystallography. *Science* **274**, 1726-1729.
Sriram, R., Kreutzer, U., Shih, L. and Jue, T. (2008). Interaction of fatty acid with myoglobin. *FEBS Lett.* **582**, 3643-3649.
Stockard, T. K., Levenson, D. H., Berg, L., Fransioli, J. R., Baranov, E. A. and Ponganis, P. J. (2007). Blood oxygen depletion during rest-associated apneas of northern elephant seals (Mirounga angustirostris). *J. Exp. Biol.* **210**, 2607-2617.
Strandberg, B. (2009). Chapter 1, Buidling the ground for the first two protein structures: myoglobin and haemoglobin. *J. Mol. Biol.* **392**, 2-10.
Teng, T. Y., Srajer, V. and Moffat, K. (1994). Photolysis-induced structural changes in single crystals of carbonmonoxy myoglobin at 40 K. *Nat. Struct. Biol.* **1**, 701-705.
Teng, T. Y., Srajer, V. and Moffat, K. (1997). Initial trajectory of carbon monoxide after photodissociation from myoglobin at cryogenic temperatures. *Biochemistry* **36**, 12087-12100.
Tilton, R. F., Jr and Kuntz, I. D., Jr (1982). Nuclear magnetic resonance studies of xenon-129 with myoglobin and hemoglobin. *Biochemistry* **21**, 6850-6857.
Tilton, R. F., Jr, Kuntz, I. D., Jr and Petsko, G. A. (1984). Cavities in proteins: structure of a metmyoglobin-xenon complex solved to 1.9 A. *Biochemistry* **23**, 2849-2857.
Tomita, A., Sato, T., Ichiyanagi, K., Nozawa, S., Ichikawa, H., Chollet, M., Kawai, F., Park, S. Y., Tsuduki, T., Yamato, T. et al. (2009). Visualizing breathing motion of internal cavities in concert with ligand migration in myoglobin. *Proc. Natl. Acad. Sci. USA* **106**, 2612-2616.
Weber, R. E. and Pauptit, E. (1972). Molecular and functional heterogeneity in myoglobin from the polychaete *Arenicola marina* L. *Arch. Biochem. Biophys.* **148**, 322-324.
Wittenberg, J. B. (1970). Myoglobin-facilitated oxygen diffusion: role of myoglobin in oxygen entry into muscle. *Physiol. Rev.* **50**, 559-636.
Wittenberg, J. B. and Wittenberg, B. A. (2003). Myoglobin function reassessed. *J. Exp. Biol.* **206**, 2011-2020.
Wyman, J. (1966). Facilitated diffusion and the possible role of myoglobin as a transport mechanism. *J. Biol. Chem.* **241**, 115-121.